Deep Machine Learning-based AoD Map and AoA Map Construction for Wireless Networks

Ronghong Mo, Yiyang Pei, Sumei Sun, A. B. Premkumar, Neelakantam V Venkatarayalu
Singapore Institute of Technology, 10 Dover Drive, Singapore 138683
Email:{ronghong.mo, yiyang.pei, sumei.sun,benjamin.premkumar, n.venkat}@singaporetech.edu.sg

2024 IEEE 99th Vehicular Technology Conference (VTC2024-Spring) | 979-8-3503-8741-4/24/$31.00 ©2024 IEEE | DOI: 10.1109/VTC2024-SPRING62846.2024.10683141

***Abstract*—Channel knowledge map (CKM) has been envisioned as a promising technology to achieve environment-aware communications for future sixth-generation (6G) wireless networks. The angle of departure (AoD) and the angle of arrival (AoA) are crucial parameters of CKM widely used for location-specific applications. Conventional stochastic methods of characterization fail to correlate the AoD and AoA with location-specific transmission environments. In this paper, we propose to utilize the CKM technology to characterize the location-specific AoD and AoA, by constructing the AoD and AoA map based on sparse measurement data. We further leverage the data-driven deep machine learning (DML) technique to obtain the AoD and AoA for locations without measurements. Simulation results show that the proposed method can construct both the AoD and the AoA maps with high fidelity to the true map. Moreover, Method II which predicts AoDs and AoAs sequentially achieves better performance than the independent prediction in Method I.**

***Index Terms*—deep machine learning, channel knowledge map, AoD, AoA, geo-location.**

I. Introduction

Channel knowledge map (CKM) is a key technology to enable environment-aware communications for future 6G networks. It provides insightful location-specific information on radio transmission environments, without the need of real-time transmission of reference signals [1]–[3]. In general, CKM is a central repository database containing location-specific information such as the pathloss, path gains, AoD, and AoA [2], [4].

AoD and AoA are parameters referring to the directions of propagation of radio signals with respect to the transmit receive antennas. AoD and AoA determine the transmit antenna response and the receive antenna response, respectively, which are combined with the complex path gains and pathloss to generate the overall wireless channel gains. AoD is essential to direct the transmit signals toward specific users or regions [5], whereas AoA is critical in positioning of devices and receive beamforming design [6].

Stochastic modelling is the conventional approach to characterize AoD and AoA, utilizing the probability distributions built from extensive research [7]. However, although it is mathematically tractable, stochastic modeling does not explicitly relate the AoD and AoA to their location-specific transmission environments such as the geographical terrain features and the city landscape. Alternatively, we can apply the CKM technique to characterize the location-specific AoDs and AoAs, e.g., the AoD map and the AoA map. The challenge of constructing these maps is to obtain the AoD and the AoA at locations without measurements. This becomes more challenging when the architecture of wireless networks gets denser, especially for future 6G networks.

Prior to the breakthrough in the DML technique, AoD and the AoA at locations with no measurement data are predicted by interpolating measurement data at known locations [8]–[10]. Recently, intensive studies have shown that data-driven DML-based methods achieved better performance than stochastic modelling in the CKM construction [11]–[13]. Although there are plenty of research works on the DML-based constructions of pathloss map [12]–[15], there are only a few works on the construction of AoD and AoA maps [16]. The AoD of the strongest path is predicted in [16] exploiting the DML technique given the locations of users, which is then used for the design of transmit beamforming.

Normally, in the wireless transmission environments, due to the presence of scattering, diffraction and refraction, there usually exist a number of paths along which the signal travels from the transmitters to the receivers. These paths, each of which having a unique AoD and AoA, together contribute to the wireless channels. It might not be sufficient to predict the AoD and AoA for the strongest path only, in order to fully characterize the wireless channels. To this end, in this paper, we propose to utilize the DML models to construct the location-specific AoD map and AoA map, based on the measured AoDs and AoAs of the first few strongest paths at some locations. The prediction of the AoDs and AoAs at locations without measurements is cast as a regression problem using DML. We predict the AoDs and AoAs of different paths, taking into account the correlation between the AoDs and AoAs. We use available datasets generated by REMCOM' Wireless InSite software to train the DML model [17], [18]. After the DML models of AoD and AoA being developed, the AoD and AoA at locations without measurements are easily obtained as the output of the DML models.

The outline of the paper is as follows. The system model and the channel model are described in Section II. The proposed DML-based AoD and AoA map construction are presented in Section III. A comprehensive performance evaluation of the proposed AoD map and AoA map construction using pubic datasets is presented in Section V. The conclusions on this work are presented in Section VI.

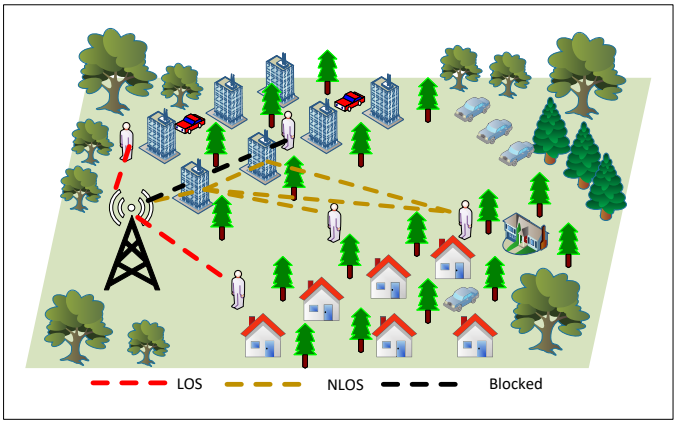

Fig. 1: A typical scenario of wireless networks with LOS, NLOS and blocked transmissions.

II. System Model

In this paper, we consider a wireless network with one transmitter (e.g., a cellular base station (BS)) whose location is known as a priori. A number of K users with the capability of AoD and AoA measurement are distributed in K locations within the coverage area. A typical scenario is shown in Fig. 1. The radio signals might propagate through environments with scattering, diffraction and refraction. As a result, at each location, the signals might experience LOS transmission, non-light-of-sight (NLOS) transmission and blockage by the surroundings.

For the k^{th} location with coordinate (x_k, y_k, z_k), we assume that there are L_k paths present between the transmitter and the receiver. Note that we have $L_k = 1$ for LOS transmission, whereas with blocked transmission we have $L_k = 0$. Given the location-dependent path parameters, following the classic geometry-based channel model, the wireless channel at the k^{th} location is given as [19]

$$\mathbf{H}_k = \sqrt{M_t M_r} \sum_{l}^{L_k} g_k^{(l)} \mathbf{a}_t^H \left(\beta_k^{(l)}, \varphi_k^{(l)}\right) \mathbf{b}_r \left(\theta_k^{(l)}, \phi_k^{(l)}\right) \quad (1)$$

where M_t, M_r are the number of antennas in the transmitter and receiver; $g_k^{(l)}$ denotes the complex path gain of the l^{th} path; $\beta_k^{(l)}, \varphi_k^{(l)}$ are the zenith and azimuth of AoD for the l^{th} path at the transmitter; $\theta_k^{(l)}, \phi_k^{(l)}$ are the zenith and azimuth of AoA for the l^{th} path at the receiver; $\mathbf{a}_t, \mathbf{b}_r$ are column vectors representing the transmit and receive antenna array response, respectively, with entries given as follows,

$$\mathbf{a}_t^{(p_t,q_t)} \left(\beta_k^{(l)}, \varphi_k^{(l)}\right) = \frac{1}{\sqrt{M_t}} e^{\frac{j2\pi d}{\lambda}\left(p_t \sin\varphi_k^{(l)} \sin\beta_k^{(l)} + q_t \cos\beta_k^{(l)}\right)} \quad (2)$$

$$\mathbf{b}_r^{(p_r,q_r)} \left(\theta_k^{(l)}, \phi_k^{(l)}\right) = \frac{1}{\sqrt{M_r}} e^{\frac{j2\pi d}{\lambda}\left(p_r \sin\phi_k^{(l)} \sin\theta_k^{(l)} + q_r \cos\theta_k^{(l)}\right)} \quad (3)$$

where $p_t = 0, \ldots, P_t - 1$ and $q_t = 0, \ldots, Q_t - 1$ with P_t, Q_t being the number of horizontal antennas and the number of vertical antennas at the transmitter; λ is the wavelength of the radio signals and d is the spacing between any two adjacent antenna elements.

Based on this model, at a given location, with the knowledge of the number of paths, path gains, AoDs and AoAs, the channel matrix $\mathbf{H}_k$ can be easily reconstructed, rather than estimated from real-time transmission of reference signals.

In this context, our objective is to build DML models, i.e., a function $f(\ )$, that maps a location $O_k = (x_k, y_k, z_k)$ to its corresponding AoD and AoA parameters $\beta_k^{(l)}, \varphi_k^{(l)}, \theta_k^{(l)}, \phi_k^{(l)}$, i.e., $\left(\beta_k^{(l)}, \varphi_k^{(l)}, \theta_k^{(l)}, \phi_k^{(l)}\right) = f(O_k)$, based on the measurements of AoD and AoA at other locations. Once built, the DML models can be used by the users to predict the AoD and AoA at locations without measurements.

Note that, the number of paths varies with location. Normally the channel matrix $\mathbf{H}_k$ can be sufficiently characterized by the first few strongest paths. Hence in the following, we target at the construction of the AoD and AoA map for the first L strongest paths, regardless of the locations.

III. DML-based AoD and AoA Map Construction

In this section, we propose two DML-based methods: Method I, sequential AoA and AoD map construction, and Method II, independent AoA and AoD map construction.

In method I, the AoD is predicted first, followed by the prediction of the AoA based on the initially predicted AoD. In total, four DML models are developed for the prediction of $\left(\beta_k^{(l)}, \varphi_k^{(l)}, \theta_k^{(l)}, \phi_k^{(l)}\right), l = 0, \cdots, L_k$. All the L_k paths are predicted together in one DML model. A simple DML model with fully connected layers only, equivalently a multi-layer perception (MLP) architecture, is employed.

For the AoD prediction, the location coordinates O_k as well as the LOS indicator I_{LOS_k}, will be input to the two DML models for the prediction of $\beta_k^{(l)}$ and $\varphi_k^{(l)}$, respectively.

For the AoA prediction, the input to the DML model will include the location coordinates, the LOS indicator and the AoD parameters, $\beta_k^{(l)}, \varphi_k^{(l)}, \forall l$. The rational behind this design is that, the AoA is indeed dependent on the AoD. Without the knowledge of the radio environments, it is expected that the knowledge of AoD can implicitly provide information of radio environments to aid the prediction of AoA.

Furthermore, there are two options in the choice of AoD data in the training of the AoA DML models, the true AoD measurement data or the predicted AoD data. In contrast, in the inference stage, the predicted AoD will be input to the AoA DML models, since the measured AoDs are not available. We will investigate the impact of AoD on the AoA prediction through simulations.

Note that, in this sequential AoD and AoA map construction, the errors in the maps constructed earlier (in this case, the AoD map) will propagate to the prediction of the AoA. Furthermore, in this paper, we assume the knowledge of the geographical terrain features and the city map is not available, the LOS indicator is therefore utilized as an overall indication of the transmission environments. The value of

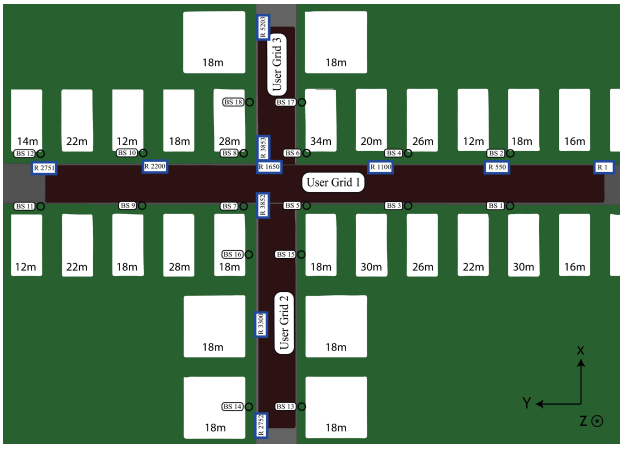

Fig. 2: The city map to generate measurement data [17].

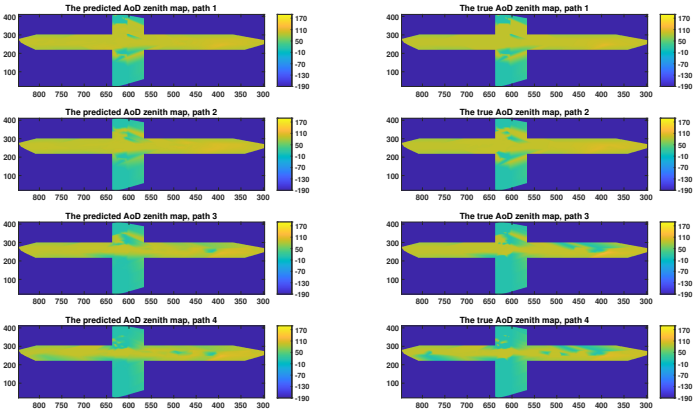

Fig. 3: The predicted and the true maps of the AoD zenith, left: the predicted maps, right: the true maps.

the LOS indicator is $1, 0, -1$, for LOS, NLOS and blocked transmission, respectively.

For comparison purposes, we consider Method II, denoted as independent AoD and AoA Map Construction. In this method, the AoD prediction remains the same as in Method I. On the other hand, the AoD map and the AoA map are constructed independently based on the O_k and I_{LOS_k}. The predicted AoD will not be used as the input to the DML model used to predict the AoA.

Compared to Method I, Method II is simple and not affected by the accuracy in the prediction of the AoD.

IV. Simulations and Performance Evaluation

In this section, we evaluate the performance of the proposed DML models for the construction of the AoD map and the AoA map using public dataset published in https://www.deepmimo.net/scenarios/o1-scenario/ [17], [18]. The performance will be evaluated in terms of the colormap and the cumulative distribution function (CDF).

A. Simulation Scenario and Data Generation

The transmission environment under consideration is shown in the Fig. 2 [17]. This is an urban outdoor scenario of area

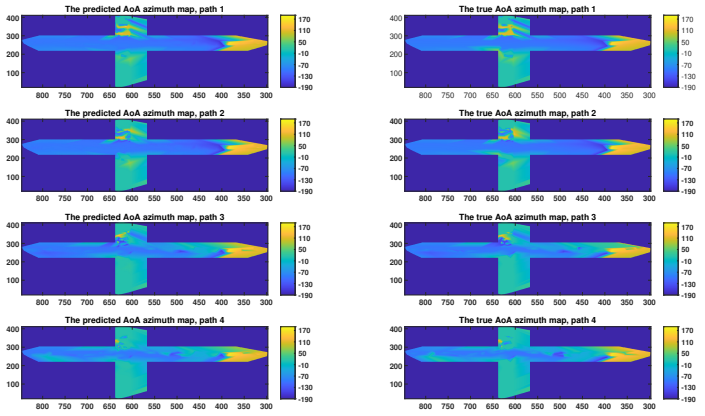

Fig. 4: The predicted and the true maps of AoA azimuth, left: the predicted maps, right: the true maps.

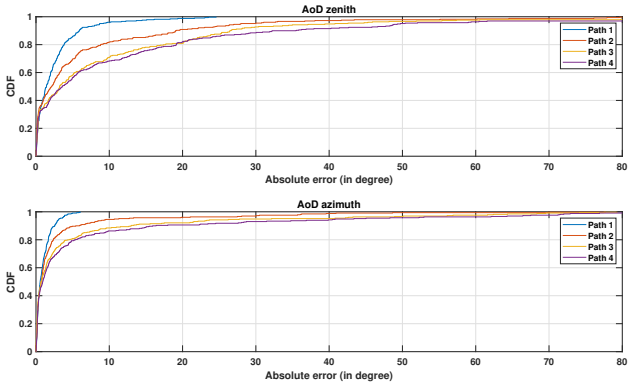

Fig. 5: The CDF of AoD zenith and azimuth.

$440m \times 600m$, with two streets, one intersection and some buildings. There are 20 BSs and more than one million users in the scenario. The height of the buildings is indicated by the number in the white blocks. In our simulations, the spacing for users in the Grid 1, 2 and 3 are around $2m$ and $15m$, $15m$ and $2m$, and $10m$ and $2m$ in the horizontal and vertical direction, respectively.

The operating frequency is 60GHz. The BSs are equipped with isotropic antennas with a height of 6 meters, whereas each user has antennas with a height of 2 meters. Each channel path can undergo a maximum of 4 reflections before reaching the receiver. The maximum number of paths is assumed to be 4. We consider the radio signal transmission from the BS1 only.

In the training of the AoD and AoA DML models, the data input to the models needs to be pre-processed by the min-max normalization. In the dataset, the number of paths varies with locations, although the maximum number of paths $L = 4$. In the case of $L_k < L$, the AoD an AoA parameters, $\beta_k^{(l)} = 10, \varphi_k^{(l)} = 10, \theta_k^{(l)} = 10, \phi_k^{(l)} = 10, \forall L_k < l <\leq L$.

We build the DML models using MLP, with 7 hidden layers, each of which has 64, 128, 256, 512, 256, 128, 64 neurons. The leakyRelu activation, Adam optimization and 0.0001 learning rate are applied when training the DML models.

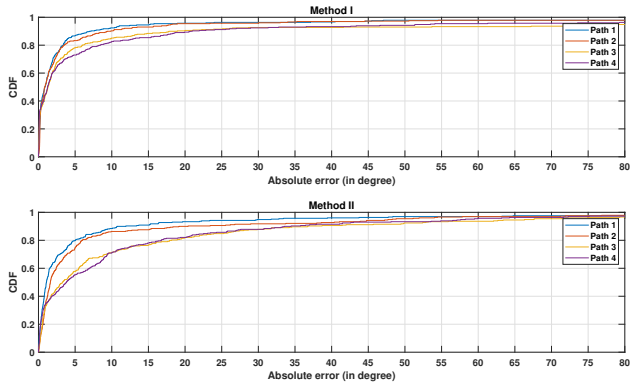

Fig. 6: The CDF of AoA zenith achieved by Method I and Method II.

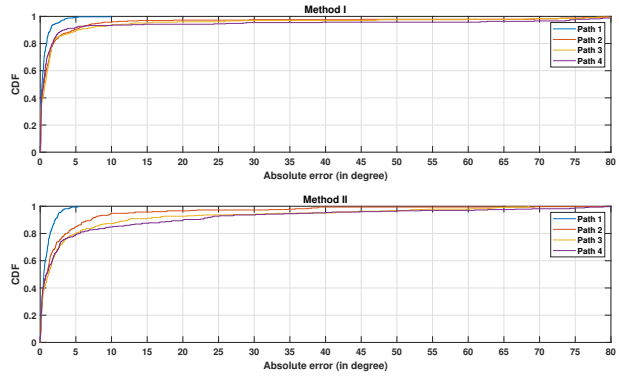

Fig. 7: The CDF of AoA azimuth achieved by Method I and Method II.

B. Performance and Observations

There are usually four maps, the AoD zenith map, the AoD azimuth map, the AoA zenith map and the AoA azimuth map. In this paper, we present only the AoD zenith map and the AoA azimuth map constructed by the proposed Method I in Fig. 3 and Fig. 4, respectively. The AoA azimuth map is constructed using the predicted AoD zenith and azimuth data for the training of the DML models. The color bars in the figures show the degrees of respective variables. The colormaps shown in the left are constructed by the proposed Method I, whereas the colormaps in the right are the true maps.

We plot the CDFs of the absolute errors between the true maps and the constructed maps by different methods in the Fig. 5 to Fig. 8.

1) Performance of AoD and AoA Maps: From the colormaps Fig. 3 and Fig. 4, it can be seen that, all the constructed maps match the true maps very well, which indicates that the proposed DML models can predict the AoD and AoA with satisfactory accuracy.

Both the CDFs of AoD shown in the Fig. 5 and the CDFs of AoA shown in Fig. 6 and Fig. 7 for Method II, represent the performance where the constructions of the maps only utilize the information of location coordinates and the LOS indicator. It can be seen that, in this case, the AoD and the AoA map construction have identical performance.

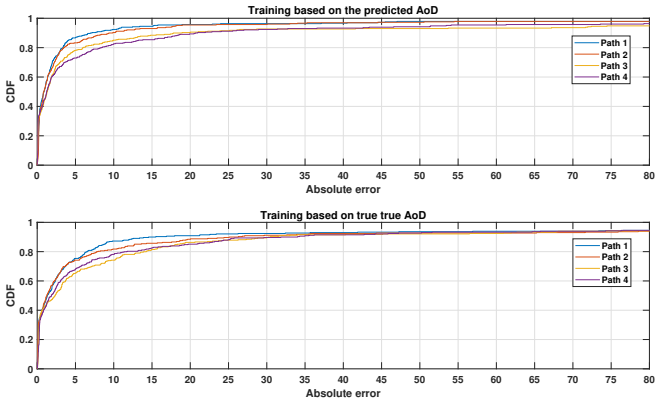

Fig. 8: The comparison of CDF of AoA zenith based on the predicted and the true AoD.

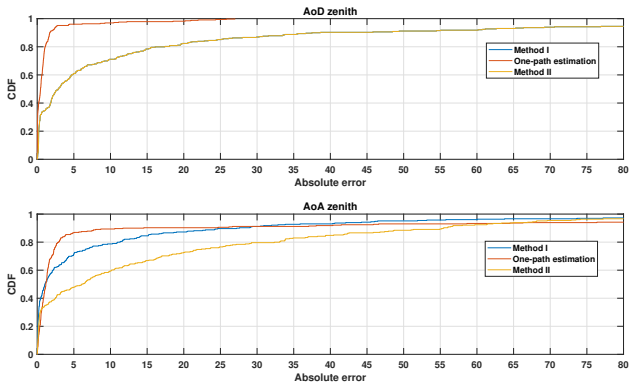

Fig. 9: The comparison of CDFs of AoA zenith by Method I, one path estimation and Method II.

2) Performance of Zenith and Azimuth: We investigate the performance of AoD zenith map and azimuth map construction in Fig. 5. We observe that the construction of the zenith map is worse than the construction of the azimuth map, for example, in the azimuth map construction of the strongest path (Path 1 in the figure), 100% of the errors being less than around 7 degrees, whereas in the zenith map construction, only 90% of the error being less than 7 degrees. This gap increases from 10% to 20% for the weaker Path 4.

These observations indicate that the DML azimuth map construction is more robust. The reason might be that the azimuth domain is less affected by the transmission environment and thus easy for the DML model to extract the features.

3) Performance of Different Paths: The maps and CDFs of different paths shown from Fig. 3 to Fig. 8 show that, the constructed maps of the strongest path (Path 1) best represent the true maps, compared to the Path 2, 3 and 4, for all the AoD zenith map, AoD azimuth map, AoA zenith map and the AoA azimuth map. This observation can be explained by the fact that the strongest path is the path least affected by the transmission environments.

4) Performance of Method I and Method II: The CDFs of errors achieved by Method I and Method II are shown in Fig. 6 and Fig. 7 for AoA map construction (note that Method I is only applicable to the AoA map construction). We notice that Method I, where the predicted AoD is used in the construction of the AoA map, achieves no worse error performance than Method II which utilizes the location information and the LOS indicator only. The performance gain increases with the weaker path, for example, for Path 1, both methods have roughly identical performance for the zenith map and the azimuth map. However, for Path 4, we can see there is a 5-degree gain for the zenith map and a 3-degree gain for the azimuth map. Hence, Method I is more favorable to the weaker paths.

5) Performance for Training on Predicted AoD and True AoD: Fig. 8 shows the CDFs of the AoA maps when the training of the DML models employs the predicted AoD map and the true map. Surprisingly, using the predicted AoD maps in the training leads to better error performance, around 4 degree gain. This is caused by the fact that, in the inference, only the predicted AoD map is available. Therefore using the predicted AoD map in the DML model training can better capture the input features.

6) Performance Comparison with Other Methods: For comparison purposes, we define another method, denoted as One-path estimation, where the DML models take the location coordinates and the LOS indicator as inputs and predict the AoD and AoA of the first path only. This is similar to the method introduced in [16] which predicts the AoD of the strongest path. Fig. 9 shows the CDFs achieved by the proposed Method I and Method II as well as the one-path estimation method. It can be seen that the one-path estimation achieves the best performance. This is because, in the one-path estimation, the DML models are optimized for the strongest path, while in our proposed Method I and Method II, the DML models are optimized for the overall loss across the four paths.

V. Conclusions

In this paper, we leverage the recently developed data-driven DML techniques to construct the location-specific AoD map and AoA map with multiple paths, based on the measured AoDs and AoAs at some locations, without explicit knowledge of channel models. The prediction of the AoDs and AoAs at locations without measurements is cast as a regression problem using DML. We consider two methods to construct the AoD map and the AoA map. In Method I, AoD is predicted first, followed by the prediction of the AoA based on the initially predicted AoD. In Method II, AoD and AoA are predicted independently of each other. Simulation results have shown that the proposed method can construct both the AoD and the AoA maps with high fidelity to the true map. Moreover, Method II which predicts AoDs and AoAs sequentially achieves better performance than the independent prediction in Method I.

Acknowledgment

This research is supported in part by the National Research Foundation, Singapore and Infocomm Media Development Authority under its Future Communications Research & Development Programme, and in part by the National Research Foundation Singapore and DSO National Laboratories under the AI Singapore Programme (AISG Award No: AISG2-RP-2020-019).

References

[1] W. Saad, M. Bennis, and M. Chen, "A vision of 6G wireless systems: applications, trends, technologies, and open research problems," *IEEE Netw.*, vol. 34, no. 3, pp. 134–142, May 2020.

[2] Y. Zeng, J. Chen, J. Xu, D. Wu, X. Xu, S. Jin, X. Gao, D. Gesbert, S. Cui, and R. Zhang, "A tutorial on environment-aware communications via channel knowledge map for 6G," *arXiv:2309.07460v1*, Sep. 2023.

[3] K. Zhang, J. Zhao, P. Liu, and C. Yin, "Radio environment map enhanced intelligent reflecting surface systems beyond 5G," in *Proc. IEEE Int. Conf. Commun. Workshops (ICC Workshops)*, June 2021.

[4] H. B. Yilmaz, T. Tugcu, F. Alagz, and S. Bayhan, "Radio environment map as enabler for practical cognitive radio networks," *IEEE Commun. Mag.*, vol. 51, no. 12, pp. 162–169, Dec. 2013.

[5] S. Kim and B. Shim, "AoD-based statistical beamforming for cell-free massive MIMO systems," in *Proc. IEEE Veh. Technol. Conf. (VTC-FALL)*, Aug 2018, pp. 267–271.

[6] N. Varshney and S. De, "AoA-based low complexity beamforming for aerial ris assisted communications at mmwaves," *IEEE*, vol. 27, no. 6, pp. 1545–1549, Apr 2023.

[7] I.-. M. P. deliverable D1.4 v1.0, *METIS Channel Models*, Feb 2015.

[8] K. Sato and T. Fujii, "Kriging-based interference power constraint: integrated design of the radio environment map and transmission power," *IEEE Trans. Cogn. Commun. Netw.*, vol. 3, no. 1, pp. 13–25, 2017.

[9] L. Bolea, J. Prez-Romero, and R. Agust, "Received signal interpolation for context discovery in cognitive radio," in *Proc. IEEE Int. Symp. Wirel. Pers. Multimed. Commun.*, Nov. 2011, pp. 1–5.

[10] D. Denkovski, V. Atanasovski, L. Gavrilovska, J. Riihijrvi, and P. Mhnen, "Reliability of a radio environment map: Case of spatial interpolation techniques," in *Proc. IEEE Int. ICST Conf. Cogn. Radio Oriented Wirel. Netw. Commun. (CROWNCOM)*, June 2012, pp. 248–253.

[11] D. Romero and S.-J. Kim, "Radio map estimation: a data-driven approach to spectrum cartography," *arXiv:2202.03269v2*, June 2022.

[12] R. Levie, C. . Yapar, G. Kutyniok, and G. Caire, "Radiounet: fast radio map estimation with convolutional neural networks," *IEEE Trans. Wirel. Commun.*, vol. 20, no. 6, pp. 4001–4015, 2021.

[13] T. Imai, K. Kitao, and M. Inomata, "Radio propagation prediction model using convolutional neural networks by deep learning," in *Proc. European Conf. Antennas Propag.*, Apr. 2019, pp. 1–5.

[14] A. Doshi, J. Namgoong, and T. Yoo, "Radio DIP - completing radio maps using deep image prior," in *Proc. IEEE Glob. Commun. Conf. (GLOBECOM)*, Dec 2023, pp. 1544–1549.

[15] S. Cen, W. Jiang, Q. Niu, and N. Liu, "FDAP: efficient radio map reconstruction using sparse signals," in *Proc. IEEE Glob. Commun. Conf. (GLOBECOM)*, Dec 2023, pp. 5919–5924.

[16] Y. Song, J. Kang, S. Kim, H. Jwa, and J. Na, "Fast beamforming strategy: Learning the aod of the dominant path," in *Proc. IEEE Int. Conf. Artif. Intell. in Info. Commun. (ICAIIC)*, Feb 2020, pp. 267–271.

[17] A. Alkhateeb, "DeepMIMO: a generic deep learning dataset for millimeter wave and massive MIMO applications," in *Proc. of Information Theory and Applications Workshop (ITA)*, San Diego, CA, Feb 2019, pp. 1–8.

[18] Remcom, "Wireless InSite," http://www.remcom.com/wireless-insite.

[19] K. Li, P. Li, Y. Zeng, and J. Xu, "Channel knowledge map for environment-aware communications: EM algorithm for map construction," in *Proc. IEEE Wirel. Commun. Netw. conf. (WCNC)*, May 2022, pp. 1659–1664.